

Technical notes

Three-dimensional fluid-suppressed T2-prep flow-independent peripheral angiography using balanced SSFP[☆]

Neal K. Bangarter^{a,*}, Tolga Cukur^b, Brian A. Hargreaves^c, Bob S. Hu^d, Jean H. Brittain^e,
Danny Park^a, Garry E. Gold^c, Dwight G. Nishimura^b

^aDepartment of Electrical and Computer Engineering, Brigham Young University, Provo, UT 84602, USA

^bDepartment of Electrical Engineering, Stanford University, Stanford, CA 94305, USA

^cDepartment of Radiology, Stanford University, Stanford, CA 94305, USA

^dPalo Alto Medical Foundation, Palo Alto, CA 94301, USA

^eGlobal Applied Science Laboratory, GE Healthcare, Madison, WI 53188, USA

Received 28 August 2010; revised 29 March 2011; accepted 4 April 2011

Abstract

Accurate depiction of the vessels of the lower leg, foot or hand benefits from suppression of bright MR signal from lipid (such as bone marrow) and long-T1 fluid (such as synovial fluid and edema). Signal independence of blood flow velocities, good arterial/muscle contrast and arterial/venous separation are also desirable. The high SNR, short scan times and flow properties of balanced steady-state free precession (SSFP) make it an excellent candidate for flow-independent angiography. In this work, a new magnetization-prepared 3D SSFP sequence for flow-independent peripheral angiography is presented. The technique combines a number of component techniques (phase-sensitive fat detection, inversion recovery, T2-preparation and square-spiral phase-encode ordering) to achieve high-contrast peripheral angiograms at only a modest scan time penalty over simple 3D SSFP. The technique is described in detail, a parameter optimization performed and preliminary results presented achieving high contrast and 1-mm isotropic resolution in a normal foot.

© 2011 Elsevier Inc. All rights reserved.

Keywords: SSFP; Peripheral angiography; Fluid suppression

1. Introduction

Interest in performing MR angiograms of the distal peripheral vasculature has increased as surgical bypass procedures have become more common in the infrapopliteal and pedal arteries. While X-ray angiography can provide most required information for surgical planning in the peripheral vasculature, it is an invasive procedure that can fail to depict clinically significant run-off vessels [1]. Imaging of peripheral vascular structure necessitates high spatial resolution given the small arterial diameters in the extremities. Contrast-enhanced MR angiography techniques,

which capture contrast during the relatively short window of time between arterial and venous enhancement, achieve limited spatial resolution.

Flow-independent angiography (FIA) techniques have been shown to be effective at producing high-resolution peripheral angiograms [1–4]. These techniques exploit the inherent differences in tissue T1, T2 and chemical shift to generate contrast, rather than rely on parameter changes induced by contrast agents. FIA without contrast enhancement is therefore not limited in spatial resolution by the short period of time between arterial and venous contrast enhancement.

Recent work has shown that the high signal-to-noise ratio (SNR), short scan times and flow properties of balanced steady-state free precession (SSFP, True FISP or FIESTA) make it an excellent candidate for angiography [5–7]. However, the characteristic large-T2/T1 fluid signal of balanced SSFP can obscure vascular structures when fluids such as edema or synovial fluid are present in the region of interest. Balanced SSFP angiograms of the pedal arteries, for

[☆] This work was supported by NIH-HL39297, NIH T32 HL07846, NIH AR46904, the State of California TRDRP 9RT-0024, Stanford University Graduate Fellowship Program and GE Healthcare.

* Corresponding author. Tel.: +1 801 422 4869, +1 650 714 8406 (mobile).

E-mail address: nealb@ee.byu.edu (N.K. Bangarter).

example, suffer from bright synovial fluid signal between the bones of the foot. Angiograms of the lower leg or extremities in patients with peripheral swelling may be obscured by bright signal from edema.

In this work, a fast, magnetization-prepared 3D SSFP sequence for creating high-resolution flow-independent angiograms with long-T1 fluid suppression is presented. The sequence exploits inversion recovery and T2 preparation combined with square-spiral centric phase encode ordering for contrast generation. Fat suppression is achieved through phase-sensitive SSFP reconstruction [8]. An analysis and optimization of scan parameters are performed to achieve fluid suppression and high arterial/muscle and arterial/venous contrast, at only a modest scan time penalty over 3D SSFP with no magnetization preparation.

2. Methods

A diagram of our 3D fluid-suppressed T2-prep SSFP pulse sequence is shown in Fig. 1. A nonselective 180_x° inversion pulse is followed by a large gradient spoiler to dephase any residual transverse magnetization. An inversion delay of length TI follows, chosen to attenuate long-T1 fluids. A TI of approximately 2 s returns both blood ($T1 \approx 1$ s) and muscle ($T1 \approx 850$ ms) to near-equilibrium values.

At the end of the inversion delay, a T2-preparation sequence is played to suppress muscle signal and enhance arterial/muscle and arterial/venous contrast [9,10]. A centric phase-encode ordering in SSFP results in image contrast exhibiting more proton-density weighting than the steady-state T2/T1 contrast typical of SSFP [11]. Use of a T2-preparation sequence generates the higher T2 discrimination needed for flow-independent angiography [12]. The sequence presented here employs a simple 90_x° , 180_y° , 180_y° , -90_x° preparation, with the echo time TE_{prep} measured between the isocenters of the first pulse (90_x° tip down) and final pulse (-90_x° tip up). The two 180_y° pulses are centered at delays of $TE_{prep}/4$ and $3TE_{prep}/4$, respectively, after the initial tip down. The final tip-up pulse is immediately followed by a gradient spoiler to dephase residual transverse magnetization.

A linear ramp start-up is performed to reduce transient oscillations immediately prior to SSFP data acquisition [13,14]. Square-spiral phase encode ordering is used to capture the prepared contrast at low spatial frequencies [15]. The square-spiral ordering was chosen for ease of implementation; an elliptical centric ordering [16] may also be used, but should yield similar results when the FOV in each of the two phase-encode directions is similar.

The above series (IR, T2-prep, catalyzation, balanced SSFP acquisition) can be repeated several times if needed during acquisition of the volume of interest, as the magnetization-prepared signal levels evolve to the steady state. In particular, the high spatial frequency artifact from long-T1 fluids is more severe as the total number of magnetization-preparation steps is decreased. When multiple repetitions are used, the sequence interleaves the square-spiral phase encodes as shown in Fig. 2. This effectively increases the extent of k -space acquired before signal levels evolve from their magnetization-prepared state to the steady state, decreasing high spatial frequency artifact. A recovery time of at least several seconds is required between each set of acquisitions to allow the volume to reach near equilibrium prior to the subsequent inversion. Thus, increasing the number of interleaves carries a concomitant penalty in scan time.

Single-cycle phase-sensitive fat detection was employed in the results presented to null fat pixels [8]. Note that single-cycle phase-sensitive fat detection is only effective if off-resonance variations across the field of view fall within a single SSFP spectral passband. Otherwise, fat pixels may drift into the water passband and have phase that is indistinguishable from water pixels. Achieving an adequate shim is therefore essential to avoid serious artifact from mistakenly identified fat and water pixels. This can be a challenge, particularly in the foot, where irregular geometry may lead to large susceptibility-induced field variations. While an adequate shim was achieved in the test cases presented to enable the use of the single-cycle fat detection method, better sequence robustness to off-resonance and improved SNR may potentially be achieved with dual-cycle phase-sensitive fat detection at the cost of doubled scan time [17].

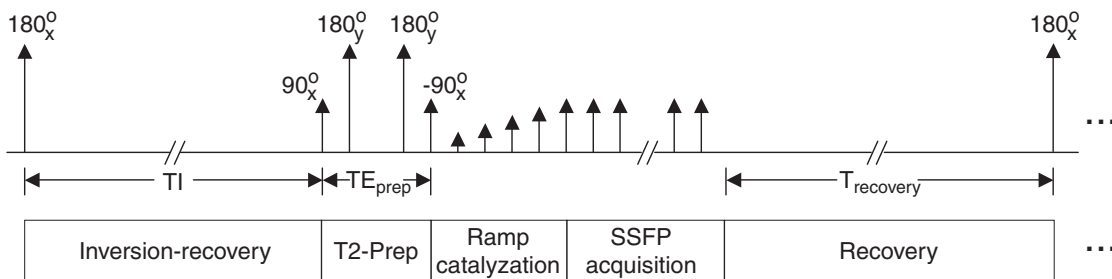


Fig. 1. Diagram of 3D IR/T2-prep SSFP sequence. A spoiled nonselective inversion is followed by an inversion time (TI), after which a T2-preparation sequence is applied. Immediately following the T2 preparation, a linear ramp catalyzation is performed to reduce transient signal oscillations. SSFP acquisition then begins, with a centric phase-encode ordering. The whole sequence is then repeated for the desired number of interleaves.

Centric Phase-Encode Interleaving (4 interleaf case)

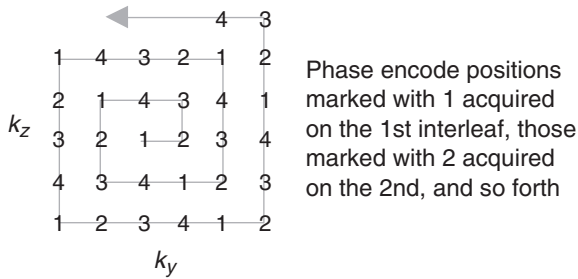


Fig. 2. Centric phase-encode interleaving. If more than one magnetization preparation is acquired to achieve good fluid suppression or T2 contrast, the square-spiral phase encodes are interleaved. The four-interleaf case is shown.

Finally, Bloch simulations of the inversion-recovery T2-prep SSFP signal evolution for on-resonant spins were performed across a range of scan parameters [18]. Values for inversion time (TI), T2-prep echo time (TE_{prep}) and flip angle (α) were selected based on these simulations, under the assumption that dominant contrast is determined by the SSFP signal levels of each tissue when the center of k -space is sampled. Results of this analysis and parameter optimization are presented below. All simulations were implemen-

ted in Matlab (The MathWorks, Natick, MA, USA). Tissue relaxation times assumed in the simulation were as follows: $T1/T2=4000/2000$ ms for synovial fluid, $1000/200$ ms for arterial blood, $1000/100$ ms for venous blood, $870/47$ ms for muscle and $270/85$ ms for fat [1,3,4].

3. Results

3.1. Analysis and parameter optimization

Bloch simulations of the SSFP signal evolution for on-resonant spins are shown in Fig. 3 for a variety of cases. In (A), the signal evolution with a simple catalyzation but no magnetization preparation is shown. The addition of an inversion-recovery preparation prior to SSFP excitations yields the signal evolution shown in (B). Signal progression after a T2-preparation pulse (with no inversion recovery) is shown in (C), while the combination of inversion-recovery and T2-prep yields (D). Pulse sequence parameters are summarized in the figure caption.

From the graphs, it is clear that the signal evolves during the course of image acquisition. Again, the assumption was made that dominant contrast is determined by the signal levels when the center of k -space is sampled. The sequence under consideration (catalyzed IR/T2-prep SSFP) makes use

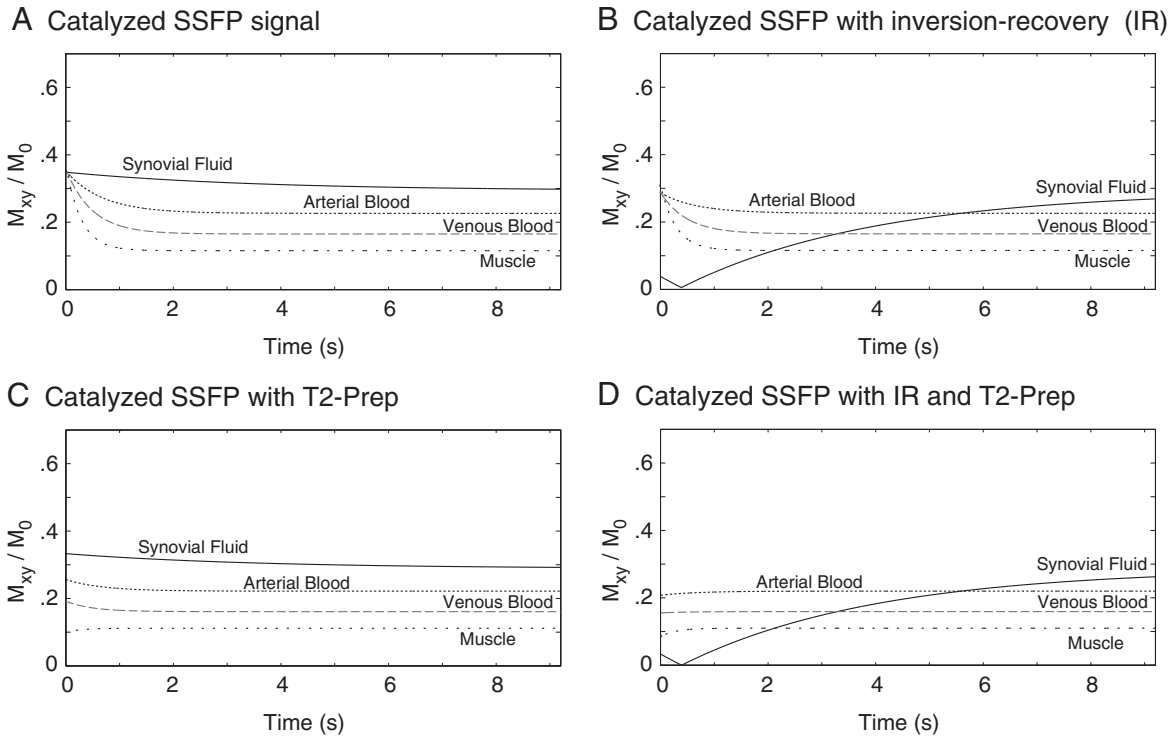


Fig. 3. Bloch simulation of catalyzed SSFP signal evolution for on-resonant spins. Simple catalyzed SSFP with no magnetization preparation is shown in (A), exhibiting consistently high signal from synovial fluid. The results of different magnetization-preparation combinations prior to SSFP imaging are shown in (B), (C) and (D). A square spiral centric phase-encode ordering ensures that dominant image contrast is given by the initial signal levels in each graph. As shown in (D), a combined IR/T2-preparation scheme can effectively null long-T1 fluid signal and set initial muscle and blood signals to near-equilibrium values. Simulation assumed $TI=2.4$ s, $TE_{prep}=60$ ms, $TR/TE=4.6/2.3$ ms and flip angle $\alpha=40^\circ$.

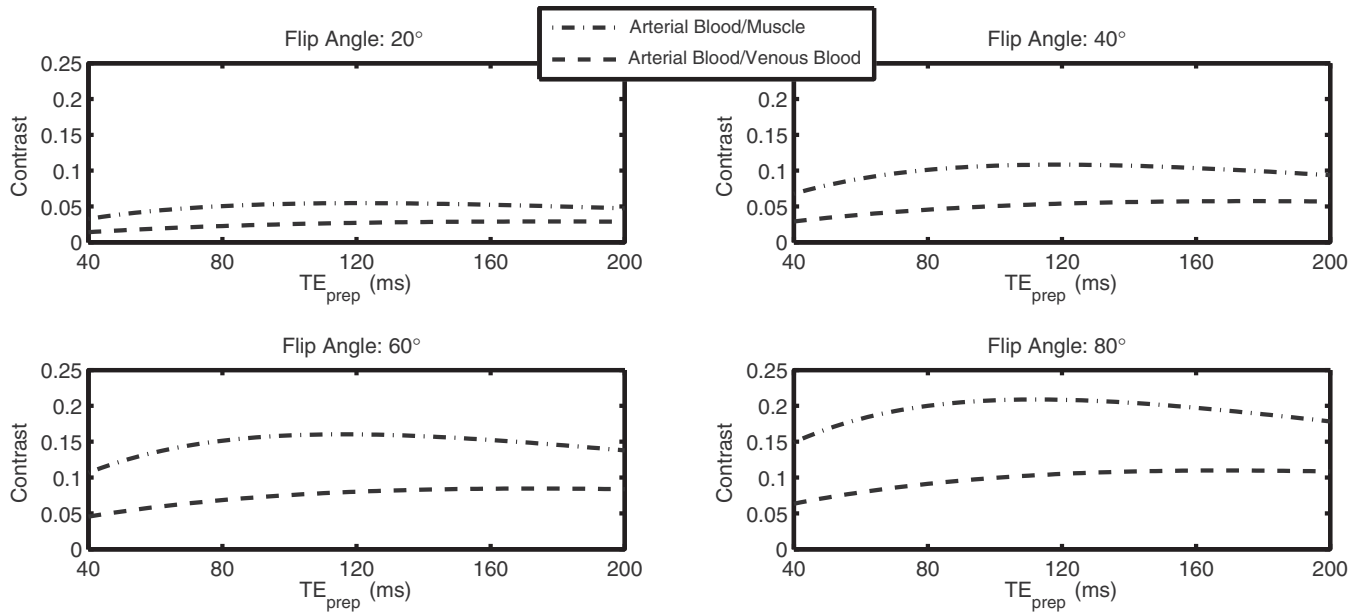


Fig. 4. Bloch simulation of IR/T2-prep SSFP contrast. The contrast achieved in IR/T2-prep SSFP is a function of TI, T2-prep echo time TE_{prep} and flip angle α . Arterial blood/venous blood contrast and arterial blood/muscle contrast are shown above as a function of TE_{prep} for flip angles of 20°, 40°, 60° and 80° at TI=2.0 s. Note that higher flip angles tend to yield better arterial/muscle and arterial/venous separation. Simulations were performed at TR/TE=4.6/2.3 ms.

of a centric phase-encode ordering (see [Methods](#)) so that contrast is roughly defined by the initial signal values in the graph shown in [Fig. 3D](#). Variations in TI, T2-prep echo time (TE_{prep}) and flip angle (α) all affect the initial signal values.

A TI of between 2 and 2.5 s was found to yield good suppression of synovial fluid. Bloch simulations were then performed with TI in this range to ascertain the initial contrast-defining signal levels as a function of TE_{prep} and α , informing parameter selection. Specifically, arterial/muscle and arterial/venous contrast were examined. Results at TI=2 s are shown in [Fig. 4](#). The graphs show simulated arterial blood/venous blood and arterial blood/muscle contrast for TE_{prep} ranging from 40 to 200 ms and flip angle values of 20°, 40°, 60° and 80°. Note that higher flip angles tend to yield better contrast, with optimal TE_{prep} values lying between about 60 and 120 ms. Simulations were performed at TR/TE=4.6/2.3 ms. The studies presented employed TI=2 s, TE_{prep} =80 ms and α =70°. The flip angle was not increased beyond 70° due to RF power deposition considerations.

3.2. In vivo results

The sequence was implemented on a 1.5-T Signa scanner (GE Healthcare, Waukesha, WI, USA) with CV/i gradients (40 mT/m maximum amplitude, 150 mT/m per millisecond slew rate). A protocol suitable for the lower leg and foot was prescribed with the following scan parameters: TR/TE=4.6/2.3 ms, α =70°, 384×128×128 matrix, 1 mm isotropic resolution, TI=2 s, TE_{prep} =80 ms and a 10-s excitation linear ramp catalyzation. Four interleaves were performed (i.e., four magnetization preparations were applied over the course

of the scan). Total scan time for the protocol was 1 min 55 s (including a long $T_{recovery}$ of 10 s to avoid gradient overheating), compared to a normal balanced SSFP scan time with the same parameters of 1 min 15 s. Imaging of all volunteers was conducted according to the ethics guidelines of Stanford University.

[Fig. 5](#) shows the results in a normal foot. The image on the left ([Fig. 5A](#)) was acquired with only the T2-prep pulse, eliminating the inversion-recovery preparation. Bright synovial fluid signal is seen in the joints of the foot, obscuring vascular structure. [Fig. 5B](#) shows the corresponding result when both the inversion recovery and T2 preparation were applied. Synovial fluid signal is well suppressed (synovial fluid SNR drops from 184 in the T2-prep-only dataset to 42 in the IR/T2-prep dataset) allowing much better visualization of the vessels. High arterial/venous contrast is also achieved by both techniques (arterial blood/venous blood contrast-to-noise ratio=42 in the T2-prep-only dataset and 39 in the IR/T2-prep dataset). The high spatial resolution allows visualization of the small caliber arteries of the foot and allows differentiation from companion vein pairs.

While the T2-prepped image clearly demonstrates the significant differences in signal intensity due to blood oxygenation difference, the elimination of longer-T2 species such as edema or synovial fluid is important. Our phase-sensitive reconstruction also performed well despite potential sensitivity in smaller vessels to partial volume effects. Finally, as predicted by simulation, there appears to be no significant loss of SNR despite the inversion pulse (arterial blood SNR=89 in the T2-prep-only dataset and 84 in the IR/T2-prep dataset).

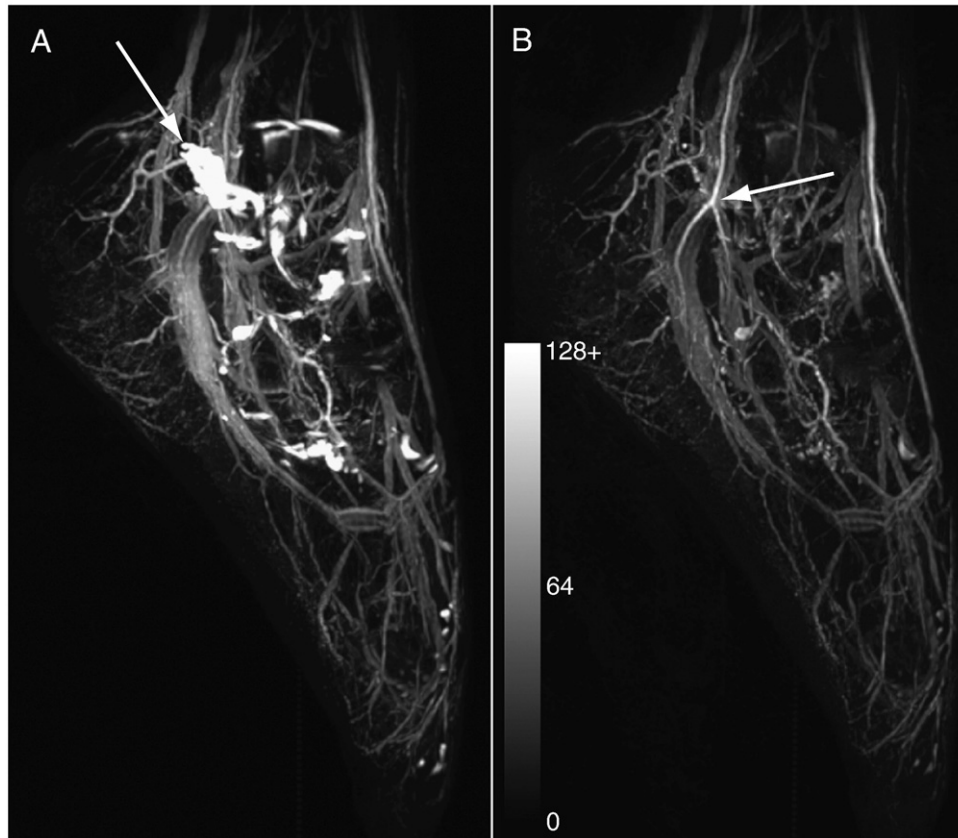


Fig. 5. Maximum-intensity projection of 3D T2-prep balanced SSFP flow-independent angiograms of the foot at 1.5 T. Phase-sensitive SSFP reconstruction was used for fat suppression. (A) Angiogram without the IR preparation (T2-prep only), showing high signal from synovial fluid in the foot joints (arrow). (B) IR and T2-prep angiogram, showing good synovial fluid suppression and high arterial/venous contrast (arrow). Both sequences employed four interleaves, a 10-excitation linear ramp catalyzation and achieve 1 mm isotropic resolution on a $384 \times 128 \times 128$ matrix. $TR/TE=4.6/2.3$ ms, $\alpha=70^\circ$, $TI=2$ s, $TE_{prep}=80$ ms. Total scan times were 1 min 47 s for (A) and 1 min 55 s for (B). Background noise level was equalized for both datasets, and the images are shown on the same intensity scale. Note, however, that the synovial fluid signal in (A) is saturating at the chosen window level.

4. Discussion

Magnetic resonance angiography of the peripheral vessels holds great promise in the visualization of small but important vessels. Compared to X-ray angiography, MR angiography avoids radiation and potential complications such as contrast nephropathy. Contrast-enhanced MR angiography has been demonstrated to be superior at detecting viable bypass targets compared to X-ray [19]. Contrast-enhanced MR angiography provides excellent vascular to other soft tissue contrast given its general suppression of all nonvascular tissue. However, the achievable resolution remains low due to the first-pass nature of the technique. Furthermore, vessels with slower flow may not be adequately visualized at all given the significant peripheral shunting that exists in patients with vascular disease. While intravascular contrast agents are being pursued vigorously, no agent has been released to date. The current flow-independent technique generates high-resolution angiography of the peripheral arteries by eliminating each of the major soft tissue signals without significantly affecting blood signal. This represents a

significant improvement over prior flow-independent angiographic techniques that rely purely on either SSFP-like contrast or T2 preparation alone.

As previously mentioned, the technique's reliance on single-cycle phase-sensitive fat detection makes it susceptible to off-resonance and partial volume effects. While careful shimming can often adequately limit off-resonance variations across the field of view, future work is needed to examine other potential ways of making the method more robust. Alternate fat suppression techniques, such as dual-cycle phase-sensitive fat detection or IDEAL (Iterative Decomposition of water and fat with Echo Asymmetry and Least-squares estimation) [20], could increase tolerance to field inhomogeneity. Preliminary work has also demonstrated the use of susceptibility-matching materials to effectively distance the air–tissue interface and increase field homogeneity across the field of view [21].

Veins are still clearly visible in the results presented. Improvements in arterial/venous contrast could possibly be achieved by going to higher field strength (3 T) and potentially increasing the TR [22,23]. However, phase-sensitive fat detection is difficult at higher field strengths, so

this would likely necessitate the use of an alternate fat-suppression technique such as IDEAL.

In conclusion, 3D magnetization-prepared balanced SSFP shows promise for rapid flow-independent angiography of the peripheral vasculature. High-resolution volumetric scans can be achieved in less than 2 min. This work has demonstrated one such sequence, employing phase-sensitive fat detection to suppress fat signal, a combined IR/T2-preparation scheme to suppress long-T1 fluid signal and improve arterial/muscle and arterial/venous contrast, and an interleaved square-spiral centric phase encode ordering to capture the prepared contrast.

References

- [1] Brittain JH, Olcott EW, Szuba A, Gold GE, Wright GA, Irrazaval P, et al. Three-dimensional flow-independent peripheral angiography. *Magn Reson Med* 1997;38:343.
- [2] Wright GA, Nishimura DG, Macovski A. Flow-independent magnetic resonance projection angiography. *Magn Reson Med* 1991;17(1): 126–40.
- [3] Wright GA, Hu BS, Macovski A. Estimating oxygen saturation of blood in vivo with MR imaging at 1.5 T. *J Magn Reson Imaging* 1991;1:275.
- [4] Gronas R, Kalman PG, Kucey DS, Wright GA. Flow-independent angiography for peripheral vascular disease: initial in vivo results. *J Magn Reson Imaging* 1997;7:637.
- [5] Deshpande VS, Shea SM, Laub G, Simonetti OP, Finn JP, Li D, et al. True-FISP: a new technique for imaging coronary arteries. *Magn Reson Med* 2001;46:494–502.
- [6] Brittain JH, Shimakawa A, Wright GA, Hargreaves BA, Han E, Stainsby JA, et al. Non-contrast-enhanced flow-independent, 3D peripheral angiography using steady-state free precession at 3T. *Proceedings of the 11th Annual Meeting of ISMRM, Toronto; 2003*. p. 1801.
- [7] Cukur T, Lee JH, Bangerter NK, Hargreaves BA, Nishimura DG. Non-contrast-enhanced flow-independent peripheral MR angiography with balanced SSFP. *Magn Reson Med* 2009;61:1533–9.
- [8] Hargreaves BA, Vasanawala SS, Nayak KS, Hu BS, Nishimura DG. Fat-suppressed steady-state free precession imaging using phase detection. *Magn Reson Med* 2003;50:210.
- [9] Brittain JH, Hu BS, Wright GA, Meyer CH, Macovski A, Nishimura DG. Coronary angiography with magnetization-prepared T_2 contrast. *Magn Reson Med* 1995;33:689–96.
- [10] Shea SM, Deshpande VS, Chung YC, Li D. Three-dimensional True-FISP imaging of the coronary arteries: improved contrast with T2-preparation. *J Magn Reson Imaging* 2002;15:597–602.
- [11] Huang TY, Huang IJ, Chen CY, Scheffler K, Chung HW, Cheng HC. Are TrueFISP images T2/T1-weighted? *Magn Reson Red* 2002;48: 684.
- [12] Shea SM, Deshpande VS, Chung YC, Li D. Three-dimensional true-FISP imaging of the coronary arteries: improved contrast with T2-preparation. *J Magn Reson Imaging* 2002;15:597–602.
- [13] Nishimura DG, Vasanawala SS. Analysis and reduction of the transient response in SSFP imaging. *Proceedings of the 8th Annual Meeting of ISMRM, Denver; 2000*. p. 301.
- [14] Hennig J, Speck O, Scheffler K. Optimization of signal behavior in the transition to driven equilibrium in steady-state free precession sequences. *Magn Reson Med* 2002;48:801–9.
- [15] Korin HW, Riederer SJ, Bampton AEH, Ehman RL. Altered phase encode order for reduced sensitivity to motion corruption in 3DFT MR imaging. *J Magn Reson Imaging* 1992;2:687.
- [16] Wilman AH, Riederer SJ. Improved centric phase encoding orders for three-dimensional magnetization-prepared MR angiography. *Magn Reson Med* 1996;36:384.
- [17] Hargreaves BA, Bangerter NK, Shimakawa A, Vasanawala SS, Brittain JH, Nishimura DG. Dual-acquisition phase-sensitive fat-water separation using balanced steady-state free precession. *Magn Reson Imaging* 2006;24:113–22.
- [18] Carr HY. Steady-state free precession in nuclear magnetic resonance. *Phys Rev* 1958;112:1693–701.
- [19] Baum RA, Rutter CM, Sunshine JH, Blebea JS, Blebea J, Carpenter JP, et al. Multicenter trial to evaluate vascular magnetic resonance angiography of the lower extremity. American College of Radiology Rapid Technology Assessment Group. *JAMA* 1995;274: 875–80.
- [20] Brittain JH, Shimakawa A, Wright GA, Hargreaves BA, Han E, Stainsby JA, et al. Non-contrast-enhanced, flow-independent, 3D peripheral angiography using steady-state free precession at 3T. *Proceedings of the 11th Annual Meeting of ISMRM, Toronto; 2003*. p. 1710.
- [21] Cukur T, DiCarlo JC, Bangerter NK, Hargreaves BA, Nishimura DG. Flow-independent angiography of the hand with 3D balanced SSFP imaging. *Proceedings of the 14th Annual Meeting of ISMRM, Seattle; 2006*. p. 1967.
- [22] Dharmakumar R, Hong J, Brittain JH, Plewes D, Wright GA. Oxygen-sensitive contrast in blood for steady-state free precession imaging. *Magn Reson Med* 2005;53:574.
- [23] Brittain JH, Shimakawa A, Wright GA, Hargreaves BA, Yang P, McConnell M, et al. Non-contrast-enhanced peripheral angiography using balanced SSFP with improved arterial-venous separation at 3T. *J Cardiovasc Magn Reson* 2004;6:503.